

Anomalous Transmission of Intense CO₂-Laser Radiation through an Overdense Plasma

Paul D. Rockett,^(a) Duncan G. Steel,^(b) John G. Ackenhusen, and David R. Bach
The University of Michigan, Ann Arbor, Michigan 48109

(Received 31 May 1977)

An ultradense ($> 10^{19} e^-/\text{cm}^3$), low-temperature (~ 20 eV), Z-pinch plasma has been used for CO₂-laser-plasma interaction experiments at $10.6 \mu\text{m}$. Anomalous transmission of radially incident, intense ($\sim 10^{11} \text{ W}/\text{cm}^2$) laser radiation of 38 nsec full width at half-maximum has been observed to occur through the initially overdense plasma. $v_{\text{osc}}/v_{\text{th}}$ is calculated to be ≈ 0.9 at the critical surface, where holographic interferometry shows critical density scale lengths of 70 to $200 \mu\text{m}$. The transmitted beam shows increased temporal modulation and a periodic spatial structure resembling Fresnel rings.

The coupling of intense laser radiation with overdense plasmas ($\omega_0 < \omega_p$) is of great importance in laser-fusion research. In particular, there is concern that CO₂ lasers (at $\lambda = 10.6 \mu\text{m}$) will produce significantly more fast electrons than Nd:glass lasers (at $\lambda = 1.06 \mu\text{m}$) because of the larger critical density radius for CO₂ lasers.¹ However, the presence of large electric fields ($v_{\text{osc}}/v_{\text{th}} \gtrsim 1$, where v_{th} is the electron thermal velocity and v_{osc} the electron quiver velocity, $v_{\text{osc}} = eE/m\omega_0$) at the critical surface has been predicted to result in significant profile modification^{2,3} reducing the critical scale length and thus reducing the energy in fast electrons. Experimental investigation of profile modification in laser-pellet plasmas is difficult and to date has largely been inferred by indirect measurements

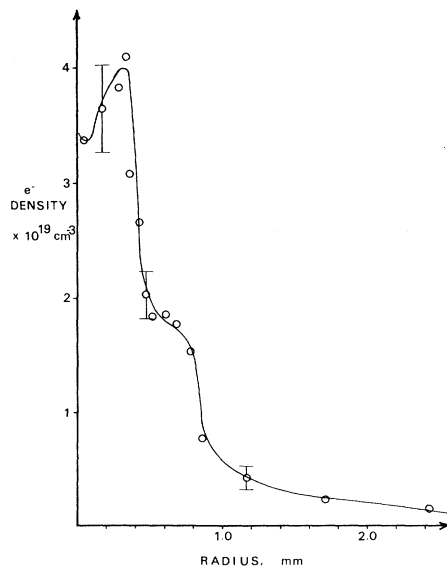


FIG. 1. Measured radial electron density profile. Obtained from Abel inversion of a holographic interferogram ($\lambda_0 = 347.2 \text{ nm}$) at peak compression.

and comparison of laser-pellet experiments and sophisticated computer codes.⁴ Direct observation of steepened density profiles in laser-pellet experiments has only recently been made.⁵ Previous experiments on independently produced plasmas with electron densities above the critical density⁶ have not had the initial steep density gradients or low electron temperatures necessary for achieving $v_{\text{osc}}/v_{\text{th}} \gtrsim 1$. In this Letter, we present preliminary results taken in this limit with an intense CO₂ laser incident on an independently produced, overdense, low-temperature helium plasma.

The plasma is a highly reproducible, small, linear, coaxial helium Z pinch discussed elsewhere.^{7,8} The discharge is 17 cm long and has an initial radius of 1.5 cm. The Z pinch is powered by a 14- μF capacitor charged to 12.75 kV, the quarter period is 2 μsec , and the time to pinch is 0.8 μsec . Peak currents are 140 kA with a total inductance of 100 nH. At maximum compression (lasting over 50 nsec) peak electron densities reach $4 \times 10^{19} \text{ cm}^{-3}$ with a critical radius

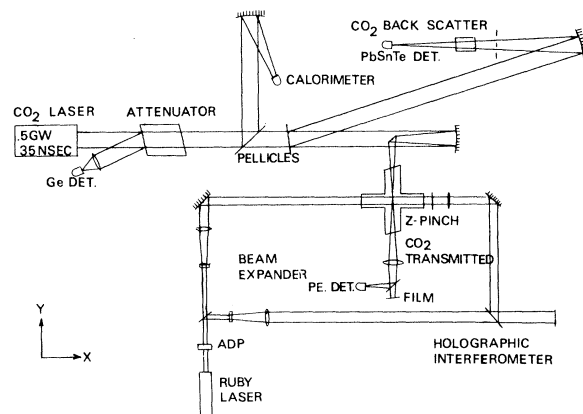


FIG. 2. Experimental configuration, shown in the X-Y plane.

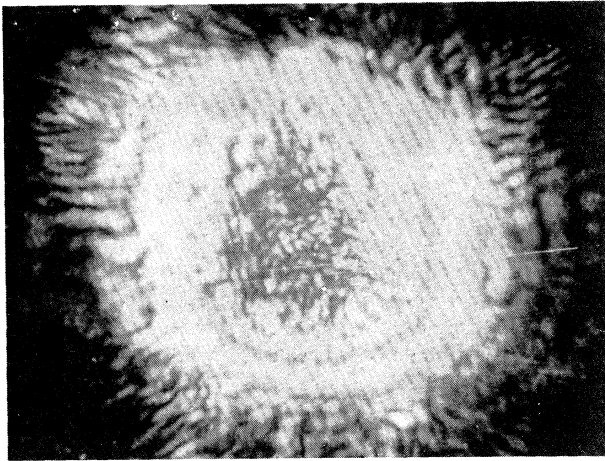


FIG. 3. Transmitted beam with no plasma present. Note annular ring characteristic of unstable resonators.

as small as $850 \mu\text{m}$ and a critical scale length ($L = N_c / \nabla N_e$) as small as $70 \mu\text{m}$ as measured by ruby-doubled holographic interferometry (see Fig. 1). These electron densities are in agreement with particle conservation if full ionization is assumed. The electron temperature is inferred from the Bennet pinch relation⁹ to be 20 eV. A lower estimate of the temperature obtained by assuming Saha equilibrium is 10 eV (at the measured density). Direct measurement of this temperature at these high densities is difficult, but the level of x-ray emission indicates that the electron temperature is below 40 eV. The independent production of this plasma has allowed us to make comparative measurements with and without the laser.

The laser is a CO_2 transverse-excitation-atmosphere laser incident on the plasma in the radial direction (rather than the z direction). Peak power is 490 MW in 38 nsec with 10–20% mode locking. The laser is equipped with an unstable resonator yielding a diffraction-limited output. Focusing is performed with a modified Newtonian copper mirror system¹⁰ giving a diffraction-limited focal spot diameter of $125 \mu\text{m}$ and a peak intensity of $2 \times 10^{12} \text{ W/cm}^2$ in vacuum. A propylene attenuator is used to vary the beam intensity.¹ Beam diagnostics include a pyroelectric calorimeter, a photon drag detector, and a PbSnTe detector used to obtain the backscattered energy. The experimental configuration is shown in Fig. 2.

Our studies have involved the investigation of forward-transmitted and/or forward-scattered beam, holographic interferograms of the interac-

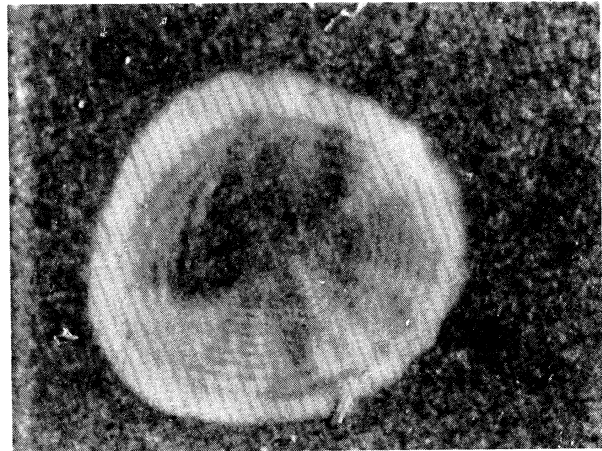


FIG. 4. Transmitted beam through an initially overdense plasma.

tion, and measurements of backscattered light. The laser intensity ranges from 10^{10} to $2 \times 10^{11} \text{ W/cm}^2$ yielding a peak $v_{\text{osc}}/v_{\text{th}} = 1$, when field swelling and collisional absorption are taken into account. Using burn photography, Fig. 3 shows the transmitted beam as recorded on film without the plasma present. The ring structure is characteristic of unstable resonators with little energy in the center. Figure 4 shows the resulting energy distribution after the beam was fired into an overdense plasma. This pattern has been observed when the beam was incident on an overdense or slightly underdense plasma, and is identical to that obtained by Fresnel diffraction through a circular aperture.¹² It should be compared to the resulting energy distribution found when the beam is incident on an underdense plasma ($N_e \approx 10^{18} \text{ cm}^{-3}$), Fig. 5. Energy measurements of the Fresnel pattern show that 4% of the incident beam is transmitted. The divergence angle of the beam transmitted through the plasma is measured to be the same as that transmitted without the plasma. This indicates that the hole produced by the laser (as deduced by the presence of the Fresnel pattern) has a diameter slightly smaller than the original focal spot, namely $125 \mu\text{m}$. Furthermore, the production of Fresnel rings requires a smooth, hard aperture. Any significant roughness in the hole would blur the rings.¹³

The presence of a critical surface indicates that significant backscatter could occur. Furthermore, at these intensities (10^{10} to $2 \times 10^{11} \text{ W/cm}^2$) parametric backscatter instabilities such as

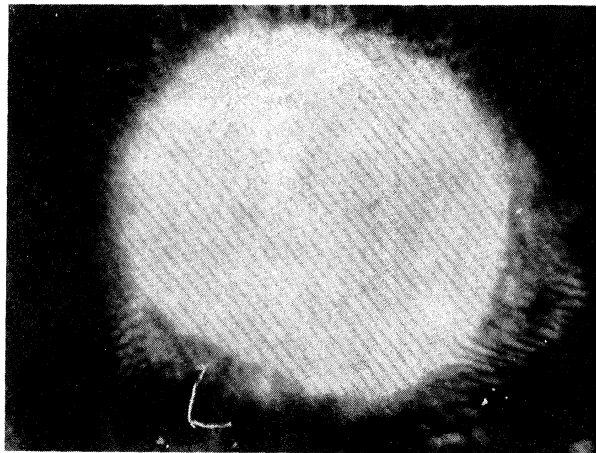


FIG. 5. Transmitted beam through an underdense ($N_e \approx 10^{18} \text{ cm}^{-3}$) plasma.

stimulated Brillouin scattering (SBS) and stimulated Raman scattering (SRS) are predicted to have significant growth rates in the infinite homogeneous plasma.^{14,15} While our backscatter detector is too slow to give time resolution of any signal with a risetime less than 65 nsec, the time-corrected integrated backscatter energy has never exceeded 0.1% over the intensity range investigated. Furthermore, the observed dependence on power is linear. Hence, we believe that to within the limits of our collection optics, we are not seeing a significant amount of backscatter energy. The absence of observed SBS or SRS is currently attributed to short temperature and density scale lengths.

The transmitted signal was time resolved using a pyroelectric detector. While the laser itself typically shows 10–20% modulation due to partial mode locking, the transmitted beam shows nearly 100% modulation on a mode-locked time scale. Furthermore, the transmitted pulse is narrower than the incident pulse, varying in width from 10 to 30 nsec (full width at half-maximum). The transmitted beam appears to occur 20–30 nsec after the laser turns on.

Holographic interferograms of the interaction have been made in an attempt to look for density modification. The spatial resolution of the existing interferometer is 200 μm , too coarse to observe directly a perturbation the size of the focal spot diameter. An example of the interaction is shown in Fig. 6. This hologram was taken 19 nsec after the beginning of the CO_2 laser pulse. This corresponded to 0.7 J incident on the plasma (a total of 1.4 J was delivered on this shot). The

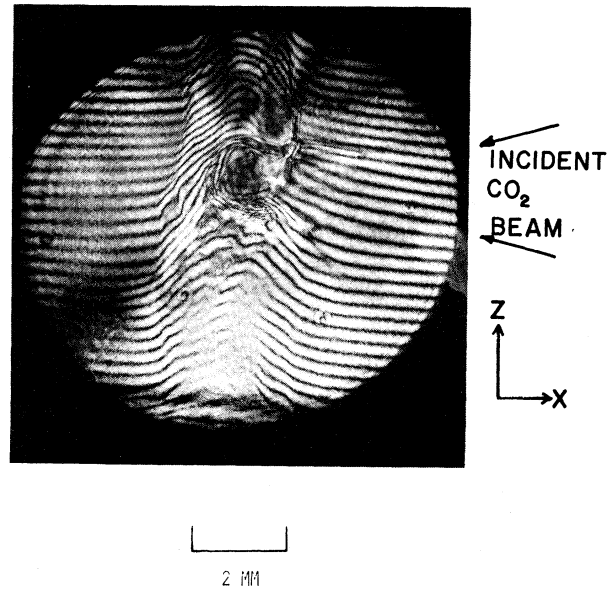


FIG. 6. CO_2 -laser-plasma interaction interferogram showing pinched plasma column along the Z axis. Overdense region extends out to a radius of 0.8 mm with a peak $n_e = 1.5 \times 10^{19} \text{ cm}^{-3}$. Time of interferogram corresponds to peak CO_2 laser intensity.

perturbed region stabilized and appeared as a density depression at the end of the laser pulse.¹⁶ It is interesting to note that if the perturbed region (i.e., that part of the hologram where the moiré pattern is lost), extending for $\Delta X = 1300 \mu\text{m}$ is assumed to be the result of thermal expansion, one can estimate the fraction of laser energy absorbed in this region assuming classical heat transfer.¹⁷ If I is the absorbed laser intensity, then energy balance requires $I\Delta t = \frac{3}{2}N_e \Delta\theta_e \Delta X$, where $\Delta\theta_e$ is the change in electron temperatures. From Fourier's law we also have that $I = K(\theta_e) \Delta\theta_e / k_B \Delta X$ where $K(\theta_e)$ is Spitzer's thermal conductivity. Using information measured from Fig. 6, we find that $\Delta\theta_e = 55 \text{ eV}$ for an initial temperature of 20 eV. This then shows a change in internal energy of approximately 0.15 J. Since the electron-ion equipartition time τ_{ei} for $\theta = 75 \text{ eV}$ is much less than Δt , the laser pulse width, we assume $\Delta\theta_e = \Delta\theta_i$. The change in kinetic energy is estimated to be 0.16 J assuming a hydrodynamic expansion velocity of $\Delta X / \Delta t$. Thus this explanation accounts for total absorbed energy of 44%.

The ratio of $\Delta X / \Delta t$ to v_{th} at this final temperature is 0.02, indicating thermal diffusion at a rate well below free-electron streaming, showing that a classical interpretation of this motion may be acceptable. It is important to note that a p - i - n

diode imaged in the plasma on the CO₂ laser focal spot shows a twofold increase in light emission (dominantly free-bound and free-free radiation) from that region at the time of the interaction.

The interaction observed in the interferograms appears to be interpretable with classical models. However, the formation of Fresnel rings is only observed when the plasma is initially overdense or slightly underdense. Currently, we are unable to explain this. Furthermore, the Fresnel pattern would indicate a quiescent state; thus, the increased modulation of the transmitted light is also unexpected. Experiments are presently underway to study the power dependence of these phenomena and to time resolve the backscatter. A subnanosecond high-power CO₂ laser is under construction so that our experiments will more nearly simulate current laser-pellet experiments.

(The formation of a hard aperture as evidenced by the Fresnel rings, and the propagation of radiation through the initially overdense plasma, have recently been predicted theoretically by Sodha and Tripathi.¹⁸)

The authors gratefully acknowledge the theoretical assistance provided by Dr. James J. Duderstadt, Dr. Donald Kenney, and Dr. Rudi S. Ong. Also, we would like to acknowledge helpful conversations with Dr. Joseph M. Kindel from Los Alamos Scientific Laboratory. This work was supported in part by the National Science Foundation, the Air Force Office of Scientific Research, and the University of Michigan College of Engineering.

^(a)Permanent address: Los Alamos Scientific Lab-

oratory, Los Alamos, N. Mex. 87545.

^(b)Permanent address: Laboratory for Laser Energetics, College of Engineering and Applied Science, University of Rochester, Rochester, N. Y. 14627.

¹Damon V. Giovanielli, *Bull. Am. Phys. Soc.* **21**, 1047 (1976).

²K. G. Estabrook, E. J. Valeo, and W. L. Kruer, *Phys. Fluids* **18**, 1151 (1975).

³D. W. Forslund, J. M. Kindel, Kenneth Lee, and E. L. Lindman, *Phys. Rev. Lett.* **36**, 35 (1976).

⁴H. G. Ahlstrom *et al.*, UCRL Report No. UCRL-77943, 1976 (unpublished).

⁵D. T. Atwood, D. W. Sweeney, J. M. Auerbach, and P. H. Y. Lee, *Bull. Am. Phys. Soc.* **22**, 1060 (1977).

⁶N. J. Peacock *et al.*, *Bull. Am. Phys. Soc.* **21**, 1039 (1976).

⁷D. G. Steel *et al.*, "An Ultradense Reproducible Z Pinch Suitable for CO₂ Laser-Pellet Simulation Experiments" (to be published).

⁸D. P. Duston, P. D. Rockett, D. G. Steel, J. G. Ackenhuisen, D. R. Bach, and J. J. Duderstadt, *Appl. Phys. Lett.* **31**, 801 (1977).

⁹M. A. Uman, *Introduction to Plasma Physics* (McGraw-Hill, New York, 1964).

¹⁰Spawr Optical Research, Inc., 1521 Pomona Rd., Corona, Calif. 91720.

¹¹R. W. MacPherson, *Rev. Sci. Instrum.* **45**, 316 (1974).

¹²M. E. Hufford and H. T. Davis, *Phys. Rev.* **33**, 589 (1929).

¹³O. P. Judd, LASL Report No. LA-5391-MS, 1973 (unpublished).

¹⁴J. F. Drake *et al.*, *Phys. Fluids* **17**, 778 (1974).

¹⁵D. W. Forslund, J. M. Kindel, and E. L. Lindman, *Phys. Fluids* **18**, 1002 (1975).

¹⁶P. D. Rockett, "Extraction of Axial Electron Density Profiles from Abel Invertible Interferograms" (unpublished).

¹⁷K. A. Brueckner and S. Jorna, *Rev. Mod. Phys.* **46**, 325 (1974).

¹⁸M. S. Sodha and V. K. Tripathi, *Phys. Rev. A* **16**, 2101 (1977).

Double-Layer Forward Shocks in a Magnetohydrodynamic Fluid

T. Tajima, J. N. Leboeuf, and J. M. Dawson

Department of Physics, University of California, Los Angeles, California 90024

(Received 19 December 1977)

We have observed forward-facing slow wave shocks created by an obstacle in a magnetohydrodynamic flow in runs on a magnetohydrodynamic particle stimulation code. The shocks have a double-layer structure composed of the compressive and accompanying rarefactive slow-wave fronts.

One of the most striking features of the magnetohydrodynamic (MHD) shocks is the possibility of a forward-facing (upstream) shock.^{1,2} Craig and Paul³ first observed in a laboratory experi-

ment slow-wave shocks in a one-dimensional configuration. Chao and Olbert⁴ inferred the existence of forward slow-wave shocks from solar wind data which showed discontinuities in physi-

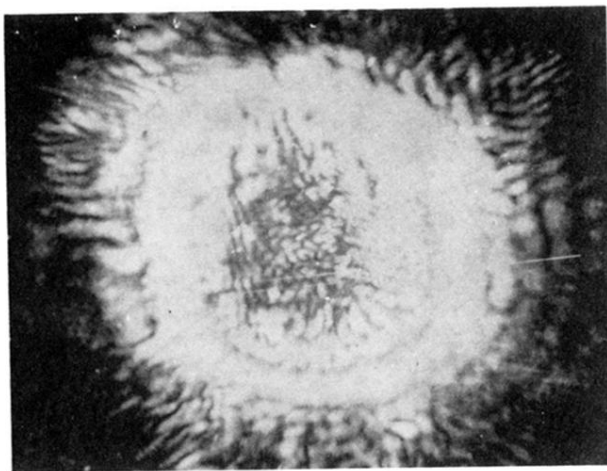


FIG. 3. Transmitted beam with no plasma present. Note annular ring characteristic of unstable resonators.

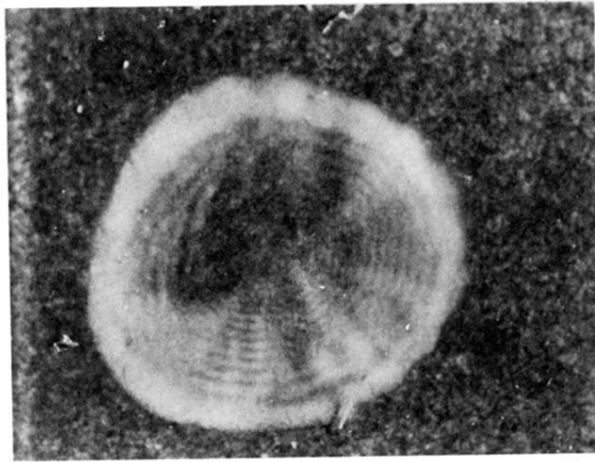


FIG. 4. Transmitted beam through an initially over-dense plasma.

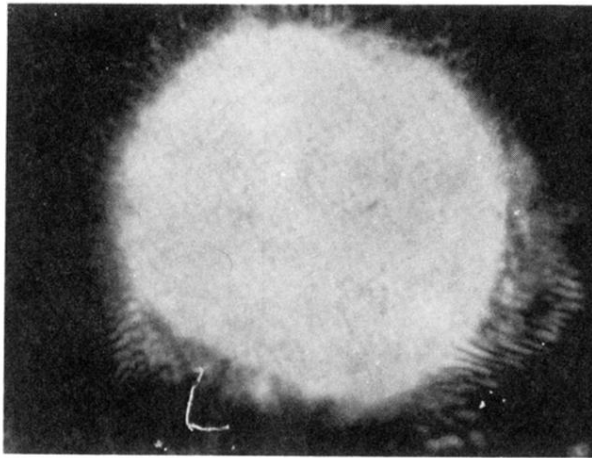
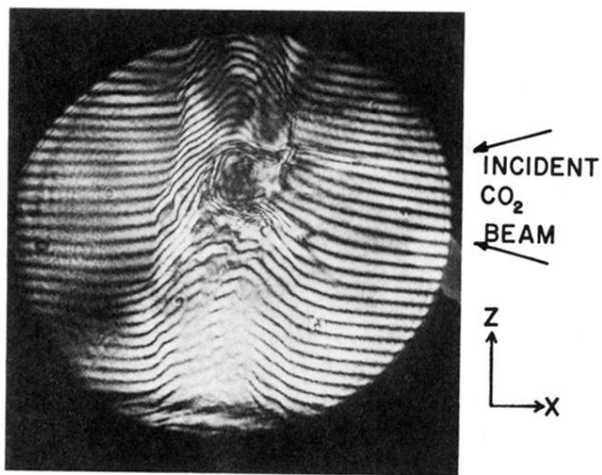


FIG. 5. Transmitted beam through an underdense ($N_e \approx 10^{18} \text{ cm}^{-3}$) plasma.



2 mm

FIG. 6. CO₂-laser-plasma interaction interferogram showing pinched plasma column along the Z axis. Overdense region extends out to a radius of 0,8 mm with a peak $n_e = 1,5 \times 10^{19} \text{ cm}^{-3}$. Time of interferogram corresponds to peak CO₂ laser intensity.